NeuroImage 188 (2019) 181–187

Contents lists available at ScienceDirect

NeuroImage

journal homepage: www.elsevier.com/locate/neuroimage

Memory entrainment by visually evoked theta-gamma coupling

Moritz Köster [a,*], Ulla Martens [b], Thomas Gruber [b]

[a] Freie Universität Berlin, Faculty of Education and Psychology, Habelschwerdter Allee 45, 14195 Berlin, Germany
[b] Osnabrück University, Institute of Psychology, Seminarstraße 20, 49074, Osnabrück, Germany

A B S T R A C T

The wake human brain constantly encodes novel information and integrates them into existing neuronal representations. It is posited that the formation of new memory traces is orchestrated by the synchronization of neuronal activity in the theta rhythm (3–8 Hz), theta coupled gamma activity (40–120 Hz), and decreases in the alpha rhythm (8–12 Hz). Critically, given the correlative nature of neurophysiological recordings, the functional relevance of oscillatory processes is not well understood. Here, we experimentally enhanced memory formation processes by a rhythmic visual stimulation at an individual theta frequency, in contrast to the stimulation at an individual alpha frequency. This memory entrainment effect was not explained by theta power *per se*, but was driven by a visually evoked theta-gamma coupling pattern. This underlines the functional role of the theta rhythm and the theta-gamma neuronal code in human episodic memory. The entrainment of mnemonic network mechanisms by a visual stimulation technique provides a proof of concept that visual pacemakers can entrain complex cognitive processes in the wake human brain.

1. Introduction

To retain a coherent internal representation of the outer world, the wake human brain constantly samples and integrates novel information from the environment, accompanying perception (Cowan, 1988). The rhythmic synchronization of neuronal activity within and across nerve cell populations is posited to coordinate and integrate distributed processes across the brain (Engel et al., 2001; Fries, 2015) and is assumed to be a key mechanism underpinning perceptual processes (VanRullen, 2016) and the integration of novel experiences into existing neuronal representations (Fell and Axmacher, 2011).

In the human brain, research has established a close association between the formation of novel memories with neuronal oscillatory activity in the theta (3–8 Hz), alpha (8–12 Hz), and gamma (40–120 Hz) frequency (Friese et al., 2013; Klimesch, 1999; Osipova et al., 2006). Specifically, successful encoding of visual stimuli was marked by increases in theta and gamma power and a decrease in alpha power (Uwe Friese et al., 2013; Osipova et al., 2006).

Theta oscillations are proposed to serve the ordering and binding of perceptual information, which are reflected in gamma synchronization processes, forming a theta-gamma neuronal code (Lisman and Jensen, 2013). This is substantiated by theta-gamma phase-amplitude coupling (PAC) processes in the human neocortex (Canolty et al., 2006), which increase in cortical and medio-temporal networks during successful memory encoding (Friese et al., 2013; Heusser et al., 2016; Köster et al., 2018; Staudigl and Hanslmayr, 2013). The theta-gamma code is assumed to facilitate the integration of perceptual information into existing networks (Buzsáki, 1996), and to promote long-term potentiation processes in the hippocampus (Köster et al., 2018; Pavlides et al., 1988). Reduced alpha oscillations during successful encoding may reflect visual perceptual and attentional gating processes (Jensen and Mazaheri, 2010; Klimesch, 2012; Köster et al., 2018).

Critically, empirical findings that fuel contemporary theoretical models on distinct roles of neuronal theta, alpha and gamma oscillations in memory encoding are foremost correlational. This is, oscillatory activity observed in the human brain could be an epiphenomenon of perceptual and mnemonic processes in neuronal networks (Buzsaki, 2004). There is first evidence that memory consolidation during sleep can be experimentally enhanced by transcranial (Marshall et al., 2006) or auditory stimulation (Ngo et al., 2013) of slow-wave delta oscillations (0.5–2 Hz). In the wake human brain, transcranial alternating current stimulation at the theta frequency (Vosskuhl et al., 2015) and with theta-gamma stimulation protocols (Alekseichuk et al., 2016) were successfully applied to enhance working memory capacity.

Regarding the encoding of visual stimuli, steady state visually evoked potentials (SSVEPs) are a fruitful method to experimentally stimulate neuronal oscillatory activity in the visual processing stream in a non-invasive way. This is, visually flickering stimuli elicit steady state visually evoked potentials (SSVEPs), an oscillatory response of the visual cortex at the specific frequency of the driving stimulus (Müller et al., 2003), which can modulate cognitive processes (Bauer et al., 2009). Importantly, a former study reported increased theta SSVEPs for

* Corresponding author. Freie Universität Berlin, Faculty of Education and Psychology, Habelschwerdter Allee 45, 14195 Berlin, Germany.
E-mail address: moritz.koester@fu-berlin.de (M. Köster).

https://doi.org/10.1016/j.neuroimage.2018.12.002
Received 18 August 2018; Received in revised form 10 October 2018; Accepted 1 December 2018
Available online 5 December 2018
1053-8119/

unfamiliar stimuli and, conversely, higher alpha SSVEPs for familiar stimuli (Kaspar et al., 2010). Furthermore, a recent audio-visual entrainment study provided first evidence that the 4 Hz theta phase of simultaneously presented auditory and visual stimuli is decisive for associative memory formation (Clouter et al., 2017). However, the authors did not further investigate the subsequent memory processes associated with memory formation by audio-visual entrainment.

In the present study, we experimentally manipulated the memory encoding process by a rhythmic visual stimulation at an individually adjusted theta rhythm to selectively enhance the memory encoding, in contrast to an individual alpha frequency, which may disrupt encoding. Individual frequencies were determined based on spectral activity during the encoding phase of a previous study (Friese et al., 2013). We further presented static stimuli to estimate the difference in memory performance for flickering and non-flickering stimuli. A scalp electroencephalogram (EEG) was recorded to test the oscillatory dynamics that predict subsequent memory performance.

2. Materials and methods

2.1. Subjects

20 university students (19 females, $M_{age} = 21.7$, $SD_{age} = 3.6$) voluntarily participated and received monetary reward or course credits. None of the subjects reported any history of neurologic or psychiatric disorders and all subjects had normal or corrected to normal visual acuity. Informed consent was obtained from all subjects and the experimental procedure agreed with the World Medical Association's Declaration of Helsinki. All subjects who returned to the laboratory from the previous study (20 of 26 subjects) were included in the analyses.

2.2. Experimental design

2.2.1. Individual frequency adjustment

We identified individual theta and alpha frequencies in the data of a preceding study. Specifically, we reinvited the subjects who participated in a previous subsequent memory experiment, which is already published (Friese et al., 2013). In this previous study we presented 300 colored object pictures, presented for 2000 ms, and subjects made living/-nonliving judgements (see the original study for details on the experimental design and data processing). The present study was conducted a few weeks after the first study.

Because theta and alpha signals vary largely across individuals (Klimesch, 1999), we selected individual frequencies on the basis of the grand mean time-frequency characteristics of the encoding phase (i.e., the spectral activity across all trials of all encoding conditions at frontal and posterior electrodes, corrected by a 500 ms pre-stimulus baseline). For each participant, the individual theta frequency was defined as the peak frequency between 3 and 8 Hz and the individual alpha frequency was defined as the trough frequency between 8 and 13 Hz, namely the alpha suppression after stimulus onset. The highest and lowest frequency was identified in the respective frequency range, in the time window from 500 to 2000 ms, to exclude event related activity. The mean individual frequencies for the 20 subjects who returned to the lab for the main study were 5.4 Hz (SD = 1.1 Hz) for theta and 10.2 Hz (SD = 1.7 Hz) for alpha. For consistency reasons, we also focused our analysis on the gamma range reported in this previous study (Friese et al., 2013), peaking at 50–80 Hz over posterior electrodes. Note that we applied the same procedure to identify individual frequencies in several previous publications (Friese et al., 2013; Köster et al., 2014, 2017a, 2017b, 2018).

2.2.2. Stimuli

The stimuli of the present experiment were 600 colored object pictures (e.g. plants, animals, clothes, tools), taken from a standard library (Hemera Photo Objects). Pictures were presented at the center of a 19 in. computer screen at a visual angle of about 6.2 × 6.2°.

2.2.3. Procedure

During encoding subjects saw 450 objects, presented in one of three conditions, in a within-subject design: individual theta, individual alpha, or static, presented in an intermixed, randomized order. Frequency stimulus allocations were counterbalanced across participants. In the theta and alpha conditions, the object was presented at the individual frequencies determined in the pre-study (see above) by controlling the presentation at every refresh cycle of a 72 Hz CRT monitor (one refresh cycle = 13.89 ms). For example, to establish a flicker rate of 6 Hz, the object was presented at a duty cycle of 6:6, i.e. six on and six off cycles. Note that we adjusted the individual frequency by using the closest theta and alpha frequency, which could be achieved with the 72 Hz monitor (namely to: 3, 3.4, 4, 4.5, 5.1, 5.5, 6.0, 6.5, 7.2, 8.0, 9.0, 10.3, or 12.0 Hz). Pictures presented statically were shown at any given duty cycle of the CRT monitor and therefore at 72 Hz (on cycles only). Each picture was presented for 3 s, following a black screen (1 s) and a white fixation dot (variable duration of 0.5–1 s), ending at a full duty cycle.

To maintain attention high during the whole stimulus presentation, subjects had to detect a magenta-colored dot that appeared for 111 ms on 15% of the encoding trials at a random time and position (including positions on the object) and respond as quickly as possible by a button press. We analyzed the detection rates and reaction times in the dot detection task (15 trials per stimulation condition) to explore potential effects of the stimulation frequency on the attention of the subjects.

The retrieval phase followed a 15 min filler task (solving simple math equations). 405 pictures from encoding were randomly intermixed with 150 new stimuli. Objects were presented for 2 s and subjects judged whether they would remember an object explicitly, with details from encoding ("remember"), the object seemed familiar ("know"), or the object was novel to them ("new"; i.e., remember/know paradigm, Tulving, 1995).

2.3. Electroencephalographic (EEG) recording

2.3.1. Apparatus

The EEG was recorded from 128 active electrodes using a BioSemi Active-Two amplifier system at 512 Hz, in a electromagnetically-shielded room. Two additional electrodes (CMS: Common Mode Sense and DRL: Driven Right Leg; cf. http://www.biosemi.com/faq/cms&drl.htm) served as reference and ground.

2.3.2. Preprocessing

EEG signals were band-pass filtered from 1 Hz to 120 Hz and segmented into epochs from −1500 ms to 4500 ms, regarding the stimulus onset. Eye-blinks and muscle artifacts were detected using an independent component procedure and removed after visual inspection. Noisy trials were identified visually and discarded (approx. 5%–10%). We applied a correction of saccade-related transient potentials (Hassler et al., 2011) to remove artifacts caused by miniature eye-movements (Yuval-Greenberg et al., 2008), before signals were re-referenced to the average reference.

2.4. Statistical analyses

2.4.1. Behavioral analysis

Given the within-subject design, we compared the pure response rates of the three stimulation conditions: subsequently remembered (SR), subsequently known (SK), and subsequently forgotten (SF) responses. Note that the response rates do not need to be corrected by false alarm rates due to the within design (i.e., correcting all conditions by the false alarm rate leads to the same within statistics). Our main comparison relied on the SR and SF responses and the subsequent memory effect (SME = SR-SF) for the theta and the alpha stimulation.

Furthermore, we tested if inter individual differences in behavioral performance would be explained by the theta or the alpha stimulation. In order to obtain a single measure for the enhancement of memory

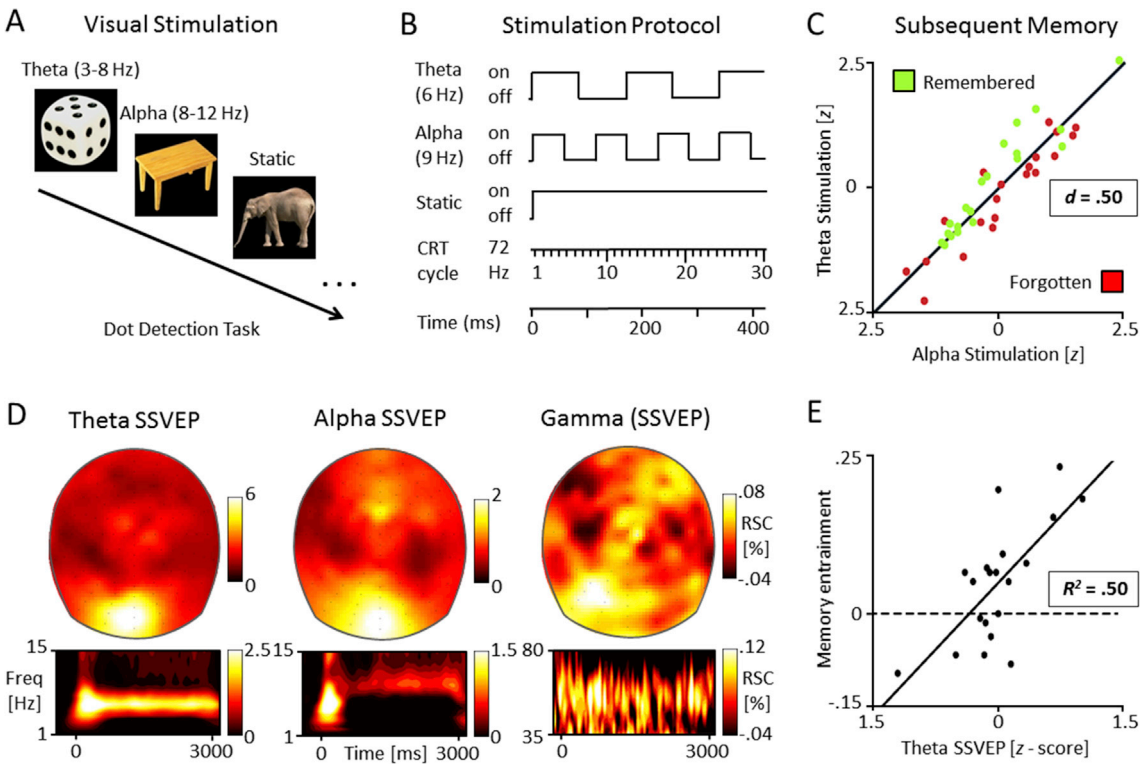

Fig. 1. Study design and visual stimulation effects on subsequent memory performance. (A) Object pictures were presented at different stimulation frequencies; individually adjusted theta (3–8 Hz), individually adjusted alpha (8–12 Hz), or static (non-flickering) during encoding. (B) Exemplary simulation protocol for the first ~400 ms for a 6 Hz theta and a 9 Hz alpha frequency and static pictures. On and off protocols refer to the refresh cycles of a 72 Hz CRT monitor. (C) Subsequently remembered (SR) and forgotten (SF) response rates are displayed (z-values used for the combined visualization). Each subject is represented by a green and a red dot. Green dots above the 45° diagonal indicate subjects with a higher SR rate for theta, red dots below the diagonal indicate subjects with a higher SF rate for alpha. The subsequent memory performance (SME = SR - SF) was higher for theta, compared to alpha ($p < .05$, Cohen's $d = 0.50$). Note that the 45° diagonal indicates equal response rates for theta and alpha stimulation and should not be confused with a regression line. (D) Topographies display the steady state visually evoked potentials (SSVEPs) at the individual theta and alpha frequency. The gamma topography displays the 50–80 Hz activity accompanying theta and alpha SSVEPs. Values indicate relative signal changes (RSC, 500–3000 ms). Time-frequency plots display the spectral power at the topographical peak electrode. (E) Inter-individual differences in the responsiveness to the visual stimulation (memory entrainment = theta SME – alpha SME) were explained by the participants theta SSVEP ($r = 0.71$, $p < .001$, $R^2 = 0.50$), but not by alpha SSVEP ($p = .697$; not displayed).

encoding by the theta compared to the alpha rhythm, we integrated the behavioral performance into one composite score, namely a memory entrainment effect (theta SME – alpha SME). To obtain a single measure for the power and spread of the theta and alpha SSVEPs, we took the mean of the SSVEP as a power measure (power at the peak electrode) and the Shannon entropy on the SSVEP values across 128 electrodes as a measure for the spread of the SSVEP signal (normalized from 0 to 1). Both measures were z-transformed (due to the different scales) and integrated into a single z-score.

2.4.2. Steady state visually evoked potentials (SSVEPs)

The main analyses focused on the SSVEPs elicited by the theta and alpha stimulation. Specifically, the evoked spectral power was obtained by Morlet's wavelets with approximately seven cycles at a resolution of 0.5 Hz for theta and alpha and a 2.0 Hz resolution in the gamma range. We identified the individual theta and alpha peak SSVEP signals, based on the grand mean spectral activity, and used the gamma range of 50–80 Hz, identified in the pre-study. Event-related changes for each condition and frequency were then calculated as the relative signal change of the post stimulus spectral activity, in percent, relative to −500 to −250 ms baseline for low frequencies, and a −200 to 100 ms baseline for gamma (Cohen, 2014). For the analysis of theta and alpha SSVEPs as well as the gamma power in the SSVEP conditions, the SSVEP grand mean peak electrode of each condition was used (Fig. 2).

2.4.3. Phase-amplitude coupling (PAC)

To assess PAC between the phase of both low frequencies, theta and alpha, and the gamma amplitude (illustrated in Fig. 2B), the modulation index (MI) (Tort et al., 2010) was calculated as described previously (Friese et al., 2013; Köster et al., 2014). Specifically, the theta and alpha SSVEPs at the grand mean peak electrodes were filtered ± 0.5 Hz around the individual peak frequency, and the gamma signal was filtered between 50 and 80 Hz, at all 128 electrodes. The MI was then calculated between the theta phase of the peak electrode in combination with the gamma amplitude, separately for each electrode, for the 500–3000 ms time window. To verify that the MI effects were not explained by power differences in the stimulated theta or the accompanying gamma rhythm, we tested the correlation between peak theta and gamma power and the average MI across all electrodes; MI and power values, split by participants and frequency conditions. With the same procedure and the same electrodes, we tested theta-gamma PAC across a 40–120 Hz gamma range, in 5 Hz steps, using a 20 Hz sliding window for the gamma frequency, separated between conditions. The resulting MI value was averaged across all electrodes. For a circular plot of the subsequent memory differences (SR-SF) for gamma amplitudes, we z-standardized the gamma amplitudes across the 18 bins for each participant and condition. The SME difference (SR-SF) in standardized gamma amplitudes was averaged over the left temporal peak electrodes of the MI difference plot (Fig. 2B).

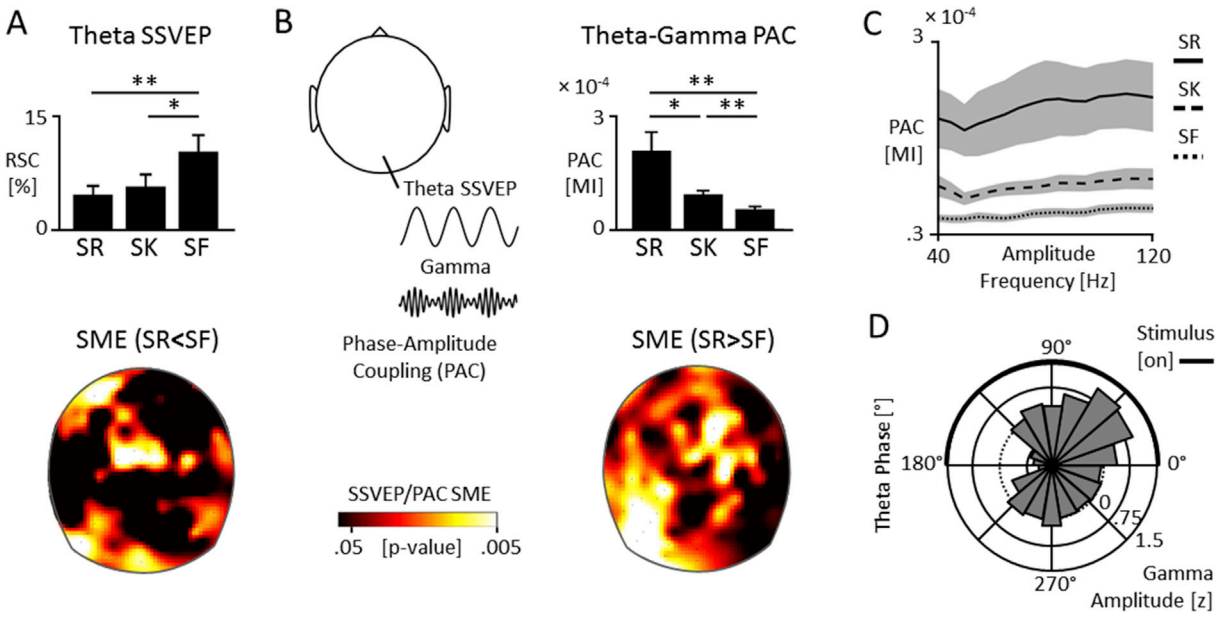

Fig. 2. Memory entrainment by theta-gamma coupling. (A) Bars indicate the theta SSVEP signal differences between subsequently remembered (SR), known (SK), and forgotten (SF) items, at the SSVEP peak electrode (ANOVA: F [2, 38] = 6.41, p = .004). The topographical map illustrates the distribution of the inverse subsequent memory effect (SME, SF > SR) across the scalp. Note that alpha SSVEP and gamma did not differ between conditions (SR, SK, SF; ps > .486, not displayed). *p < .05, **p < .01. (B) The cartoon head illustrates theta-gamma phase-amplitude coupling, between individual theta rhythm and the 50–80 Hz gamma frequency range, as assessed by the modulation index (MI). Bars display the mean differences in MI, averaged across all electrodes (F [2, 38] = 8.08, p < .001). The topographical map displays the distribution of the SME (SR > SF) in theta-gamma PAC. Note that theta-gamma PAC was much higher than alpha-gamma PAC (p < .002; not displayed). (C) Theta-gamma PAC across the 40–120 Hz gamma range. MI values indicate the mean PAC between gamma amplitude at each of 128 electrodes to the individual SSVEP theta phase at the peak electrode. (D) The circular histogram displays subsequent memory differences (SR-SF) for z-standardized gamma amplitudes at the left temporal peak electrodes of the MI difference plot.

3. Results

3.1. Visual theta and alpha stimulation effect subsequent memory performance

The stimulation at an individual theta frequency increased subsequent memory performance (SME = SR-SF), compared to the alpha stimulation, t (19) = 2.24, p = .037, Cohen's d = 0.50 (see Fig. 1C). This was due to a higher number of subsequently remembered (SR) items in the theta stimulation condition, compared to the alpha stimulation, 23.8% (SD = 16.9%) vs. 21.5% (SD = 15.7%), t (19) = 2.13, p = .046, and a higher rate of subsequently forgotten (SF) items in the alpha stimulation condition, compared to the theta stimulation, 47.4% (SD = 16.9%) vs. 49.9% (SD = 16.7%), t [19] = 1.99, p = .062, by trend. Pictures presented statically were remembered best (SR: 28.2% [SD = 16.2%] and SF: 42.6% [SD = 16.6%]), with a higher SME compared to the theta (t [19] = 4.15, p .001), and the alpha stimulation (t [19] = 10.97, p .001). SR rates were below chance (i.e., 33.3%), but markedly higher than the false alarm rate of 3.5% (SD = 4.7%), namely, remember responses to novel stimuli, indicating guesses, all t (19) > 6.02, p < .001. The stimulation condition did not affect the rates of subsequent know (SK) responses (theta: 28.7% [SD = 10.3%], alpha: 28.6% [SD = 10.0%], static: 29.3% [SD = 9.6%]). All mean differences for SR and SF were tested post hoc, following significant main effects and interactions in the overall ANOVA (3 Conditions [theta, alpha, gamma] x 3 Responses [SR, SK, SF]) and the subsidiary ANOVAs for SR and SF responses, all p < .001.

To test if the visual stimulation condition (theta, alpha, static) affected participants' attention processes during encoding, we tested for differences in dot detection performance and reaction times. Overall participants were highly attentive and detected on average 44.1 of 45 dots (97.9%), with no effect of the encoding condition, F (2, 38) = 1.30, p = .273. However, reaction times were fastest in the alpha stimulation (M = 494 ms, SD = 67 ms), and the theta stimulation (M = 508 ms, SD = 54 ms), compared to the static condition (M = 521 ms, SD = 47 ms), F (2, 38) = 7.27, p = .005, both t (19) > 2.66, p < .016. Reaction times were also marginally faster for the alpha compared to the theta stimulation, t (19) = 1.91, p = .072. Thus it is unlikely that higher memory performance for stimuli presented in theta compared to alpha, were due to differences in attention or perception during encoding.

3.2. Participants' responsiveness to the theta stimulation predicts memory entrainment

The theta and the alpha stimulation elicited clear SSVEP signals over the visual cortex, accompanied by increased gamma oscillations at posterior recording sites, all t (19) > 3.11, all p .006 (Fig. 1D). The effect size of the memory entrainment effect for theta compared to alpha was at an intermediate level and not all participants responded equally well to the visual stimulation (i.e., participants close to the 45° diagonal in Fig. 1C). Thus, we tested if inter-individual differences in participants SSVEP brain response to the visual stimulation would explain differences in the memory entrainment effect. The memory entrainment effect (theta SME - alpha SME) was clearly predicted by the power and spread of the theta SSVEP, r = .71, p = .00043, R^2 = 0.50 (see Fig. 1E), but no relation was found between the alpha SSVEP signal and the memory entrainment effect, r = 0.09, p = .697. Thus, memory entrainment was driven by memory enhancing effects of the theta stimulation, but not by disrupting effects of the alpha stimulation.

3.3. Memory entrainment is driven by visually evoked theta-gamma phase-amplitude coupling (PAC)

At the individual level, theta oscillations showed an inverse SME, namely higher theta SSVEPs for SF, than SK, than SR items (Fig. 2A, upper panel), F (2, 38) = 6.41, p = .004. This inverse SME was distributed

across posterior, central and frontal regions (Fig. 2A, lower panel). The memory enhancing effect of the theta stimulation was resolved by the theta-gamma PAC analyses. We tested the coupling between the phase of the individual theta SSVEP at the peak electrode with the 50–80 Hz gamma amplitude (Fig. 2B) at all 128 electrodes. We found a clear SME, namely higher theta-gamma PAC for SR, compared to SK, compared to SF items, when tested across all electrodes, $F\,(2,\,38) = 8.08$, $p < .001$. The difference in theta-gamma PAC was highest at left temporal and centro-frontal electrodes (Fig. 2B). In accordance with previous studies (Friese et al., 2013; Köster et al., 2014, 2018), neither theta nor gamma power was correlated with the MI coupling magnitude (theta: $r = -0.209$ $p = .108$; gamma: $r = -0.033$ $p = .803$).

Further inspection of theta-gamma PAC revealed that the SME in theta-gamma coupling was not restricted to the preselected gamma frequency range (50–80 Hz), and ranged from 40 to 120 Hz (Fig. 2C). We further looked at the critical theta phase of theta-gamma PAC for successful memory encoding at left temporal recording sites. The gamma amplitude difference (SR-SF), was specifically high at an early theta phase (0°–90°), corresponding to the onset of the flickering stimulus, but lower towards the offset of the flickering stimulus (120°–210°; Fig. 2D).

No differences between encoding conditions (SR, SK, SF) were found for the alpha SSVEPs, $F\,(2,\,38) = 0.74$, $p = .486$. Furthermore, the gamma power accompanying the SSVEP conditions (displayed in Fig. 1C), did not differ between conditions, when tested in an ANOVA with all subsequent responses (SR, SK, SF) and both SSVEP conditions (theta and alpha), all $ps > .634$, for all main effects and interactions. In addition, across all conditions and all electrodes, theta-gamma PAC was much higher than alpha-gamma PAC, $t\,(19) = 3.53$, $p = .002$. Thus, neither the alpha SSVEPs nor the accompanying gamma power as such differed between encoding conditions. Also, rehearse that inter-individual differences in memory entrainment were driven by the theta SSVEP, but not by the alpha SSVEP (see above). Because of this, the encoding activity was not further analyzed or visualized in more detail for these conditions.

4. Discussion

By entraining neuronal oscillatory activity using rhythmic visual brain stimulation, this study substantiates a functional role of the theta rhythm and provides further evidence for the theta-gamma neuronal code in human episodic memory processes (Lisman and Jensen, 2013). Specifically, subsequent memory performance was higher for a visual stimulation at an individual theta frequency, compared to a stimulation at an individual alpha frequency. This memory entrainment effect was strongest for participants with a high SSVEP response to the theta stimulation, indicating that memory entrainment was due to the visual stimulation at the theta rhythm. However, at the individual level, subsequent memory performance was not explained by the theta SSVEP *per se*, but was driven by theta-gamma PAC entrained by the theta stimulation. More generally, these results demonstrate that simplistic external pacemakers can stimulate rhythmic processes in the wake human brain and thereby entrain complex cognitive functions, such as memory.

In the theta power we found a positive effect on memory entrainment for participants SSVEP response to the theta stimulation, but an inverse SME (SR < SM) at the individual level. The latter result contradicts former findings of higher theta power during memory processes in studies analyzing non-individualized frequency ranges (Backus et al., 2016; Hanslmayr et al., 2009; Osipova et al., 2006; Sederberg et al., 2003) and using individual theta frequencies (Friese et al., 2013; Köster et al., 2017b; Köster et al., 2018). However, recently a number of studies using non-individualized frequency ranges has also revealed lower theta power for successful encoding (Burke et al., 2013; Greenberg et al., 2015; Griffiths et al., 2016). Critically, the SME in theta-gamma PAC pattern was in the expected direction (SR > SM). Thus, theta SSVEP power between participants may rather indicate if the stimulation was effective (i.e., eliciting resonant activity in neuronal networks, possibly due to a well-adjusted individual frequency), but it was then not the power as such, which entrained memory, but the specific theta-gamma dynamics elicited by theta SSVEP. This is in line with recent suggestions that the temporal structure, which the theta rhythm provides is decisive for memory binding, rather than the theta power by itself (Berens and Horner, 2017; cf. Clouter et al., 2017).

The alpha SSVEP stimulation was associated with a lower memory performance, compared to the theta stimulation. However, the alpha SSVEP signal did not explain inter-individual differences in memory entrainment and did not differ between encoding conditions (SR, SK, SF). Thus, the alpha SSVEP stimulation was unspecific compared to the visually entrained theta rhythm and theta-gamma PAC pattern. This dissociation between the theta and the alpha rhythm is in line with recent findings on the phase synchronization of theta but not alpha (nor delta) oscillations for associative memory formation (Clouter et al., 2017; Köster et al., 2018). As could have been expected, non-flickering stimuli were remembered best: This may either be due to the physically longer presentation time (no off frames), or simply because, in the absence of external stimulation, the brain could more flexibly adjust its rhythmicity. Yet another possibility would be that entrained 72 Hz, the frequency of the monitor, may have contributed to encoding. However, the present design does not allow to disentangle these possibilities. Additionally, the major part of the participants in the present study were female students. It would be favorable to replicate the findings with more heterogeneous age and gender characteristics.

The theta (3–8 Hz) versus alpha (8–12 Hz) pace of the stimulus presentation may modulate memory encoding via attention and perception processes. The analysis of accuracy and response times in the dot detection task (15% of the trials), substantiates that subjects were highly attentive for the whole 3 s time window of the stimulus presentation and that their level of attention did not differ between the theta and the alpha stimulation conditon. Furthermore, a recent audio-visual entrainment study, which also reports beneficial effects of a theta stimulation on memory encoding (Clouter et al., 2017), also controlled for a lower delta (1.7 Hz) frequency. Thus, perceptual stimulation effects in the theta rhythm are not explained by low level differences in attention or simply by a slower vs. faster stimulation speed. As a critical addition, recording a high-density EEG, we could here identify neuronal dynamics entrained by the theta stimulation that predicted subsequent memory and which cannot be due to differences between the encoding conditions. Overall, these results further underline the entrainment account of perceptual theta stimulation techniques. Yet, entrained theta oscillations may facilitate memory encoding process via rhythmical perceptual dynamics that act in concert with memory encoding processes. This would be in line with common conceptions of perception and memory as embedded processes (Cowan, 1988; Craik and Lockhart, 1972) and recent studies that highlight the role of the theta rhythm in perceptual sampling (Landau et al., 2015; Lowet et al., 2016; Spyropoulos et al., 2018; Helfrich et al., 2018), discussed in more detail below.

Importantly, we could pinpoint a subsequent memory effect for gamma oscillations that were coupled to the entrained theta rhythm, with higher theta-gamma PAC for later remembered stimuli. At the same time, we found an inverse SME in theta power and no SME in gamma power. Furthermore, like in former studies (Friese et al., 2013; Köster et al., 2014, 2018), neither theta nor gamma power was correlated with the MI magnitude. Thus, the theta-gamma PAC effects reported here, were not confounded with power differences in the theta or gamma amplitude. While time-varying input may effect PAC results (Aru et al., 2015), this could not explain the differences in PAC within the theta stimulation condition (e.g., SR vs. SF), because the time varying inputs were identical for all trials within conditions.

Theta oscillations in the cerebral cortex are associated with mnemonic control processes, the ordering and binding of perceptual information, reflected in gamma oscillations, which are nested in the theta phase (Bahramisharif et al., 2017; Heusser et al., 2016; Köster et al., 2017b; Köster et al., 2018; Lisman and Jensen, 2013). In line with this idea, we found a strong subsequent memory effect in theta-gamma PAC

and the theta stimulation selectively improved context-dependent, associative memories (SR, "remember" responses), but not familiarity based memory processes (SK, "know" responses) (Tulving, 1995). However, while the theta rhythm is ascribed a prefrontal and medio-temporal control function (Anderson et al., 2010; Backus et al., 2016; Buzsáki, 1996), the present study adds to recent evidence for a bottom-up mechanism of the theta-gamma code in the visual cortical networks (Landau et al., 2015; Lowet et al., 2016), and a specific role of the theta rhythm in perceptual sampling (Spyropoulos et al., 2018; Helfrich et al., 2018). Speculatively, the prefrontal and medio-temporal system, in concert with the oculomotor and the visual system may implement a mnemonic sampling loop. Novel perceptual information, reflected in gamma bursts, may be sampled bit by bit, at a theta pace (Fries, 2015; VanRullen, 2016), in order to integrate them into existing neuronal networks and to establish a continuous update of internal representations of the external world (Buzsáki, 1996). Specifically, theta-gamma PAC may map real time events onto a neuronal time scale, to provide an optimal temporal code for long-term potentiation processes in the medial temporal lobe (Pavlides et al., 1988), the core system for episodic memories (Squire and Zola-morgan, 1991), to establish a coherent representation of time and space (Eichenbaum, 2017).

To conclude, this is the first study to demonstrate that rhythmic visual brain stimulation can entrain complex cognitive functions, such as memory encoding, in the wake human brain. Specifically, memory entrainment was explained by participants' responsiveness to a visual stimulation at a theta pace and the present findings support the critical role of theta-gamma coupling as key mechanism in memory formation. More generally, the present findings show how visual stimulation techniques open up new ways for the selective enhancement and the investigation of functional mechanisms that underpin human cognition.

Conflicts of interest

There are no conflicts of interest.

Acknowledgements

We thank Nikolai Axmacher and Malte Wöstmann for comments on an earlier version of the manuscript.

References

Alekseichuk, I., Turi, Z., Amador de Lara, G., Antal, A., Paulus, W., 2016. Spatial Working Memory in Humans Depends on Theta and High Gamma Synchronization in the Prefrontal Cortex. Curr. Biol. 26, 1513–1521. https://doi.org/10.1016/j.cub.2016.04.035.

Anderson, K.L., Rajagovindan, R., Ghacibeh, G.A., Meador, K.J., Ding, M., 2010. Theta oscillations mediate interaction between prefrontal cortex and medial temporal lobe in human memory. Cerebr. Cortex 20, 1604–1612. https://doi.org/10.1093/cercor/bhp223.

Aru, J., Aru, J., Priesemann, V., Wibral, M., Lana, L., Pipa, G., Singer, W., Vicente, R., 2015. Untangling cross-frequency coupling in neuroscience. Curr. Opin. Neurobiol. 31. https://doi.org/10.1016/j.conb.2014.08.002.

Bahramisharif, A., Jensen, O., Jacobs, J., Lisman, J., 2017. Serial representation of items during working memory maintenance at letter-selective cortical sites (bioRxiv).

Backus, A.R., Schoffelen, J.M., Szebényi, S., Hanslmayr, S., Doeller, C.F., 2016. Hippocampal-prefrontal theta oscillations support memory integration. Curr. Biol. 26 (4), 450–457. https://doi.org/10.1016/j.cub.2015.12.048.

Bauer, F., Cheadle, S.W., Parton, A., Müller, H.J., Usher, M., 2009. Gamma flicker triggers attentional selection without awareness. Proc. Natl. Acad. Sci. U. S. A 106, 1666–1671. https://doi.org/10.1073/pnas.0810496106.

Berens, S.C., Horner, A.J., 2017. Theta Rhythm: Temporal Glue for Episodic Memory. Curr. Biol. 27, R1110–R1112. https://doi.org/10.1016/J.CUB.2017.08.048.

Burke, J.F., Zaghloul, K.A., Jacobs, J., Williams, R.B., Sperling, M.R., Sharan, A.D., Kahana, M.J., 2013. Synchronous and asynchronous theta and gamma activity during episodic memory formation. J. Neurosci. 33, 292–304. https://doi.org/10.1523/JNEUROSCI.2057-12.2013.

Buzsaki, G., 2004. Neuronal Oscillations in Cortical Networks. Science (80-.) 304, 1926–1929. https://doi.org/10.1126/science.1099745.

Buzsáki, G., 1996. The hippocampo-neocortical dialogue. Cerebr. Cortex 6, 81–92. https://doi.org/10.1093/cercor/6.2.81.

Canolty, R.T., Edwards, E., Dalal, S.S., Soltani, M., Nagarajan, S.S., Kirsch, H.E., Berger, M.S., Barbaro, N.M., Knight, R.T., 2006. High Gamma Power Is Phase-Locked to Theta Oscillations in Human Neocortex. Science (80-.) 313, 1626–1628. https://doi.org/10.1126/science.1128115.

Clouter, A., Shapiro, K.L., Hanslmayr, S., 2017. Theta Phase Synchronization Is the Glue that Binds Human Associative Memory. Curr. Biol. 27, 3143–3148 e6. https://doi.org/10.1016/j.cub.2017.09.001.

Cohen, M.X., 2014. Analyzing Neural Time Series Data: Theory and Practice. MIT Press. https://doi.org/10.1017/CBO9781107415324.004.

Cowan, N., 1988. Evolving Conceptions of Memory Storage, Selective Attention, and their Mutual Constraints Within the Human Information-Processing System. Psychol. Bull. 104, 163–191.

Craik, F.I.M., Lockhart, R.S., 1972. Levels of processing: A framework for memory research. J. Verb. Learn. Verb. Behav. 11, 671–684. https://doi.org/10.1016/S0022-5371(72)80001-X.

Eichenbaum, H., 2017. On the Integration of Space, Time, and Memory. Neuron 95. https://doi.org/10.1016/j.neuron.2017.06.036.

Engel, A.K., Fries, P., Singer, W., 2001. Dynamic predictions: Oscillations and synchrony in top–down processing. Nat. Rev. Neurosci. 2, 704–716. https://doi.org/10.1038/35094565.

Fell, J., Axmacher, N., 2011. The role of phase synchronization in memory processes. Nat. Rev. Neurosci. 12, 105–118. https://doi.org/10.1038/nrn2979.

Fries, P., 2015. Rhythms for Cognition: Communication through Coherence. Neuron 88, 220–235. https://doi.org/10.1016/j.neuron.2015.09.034.

Friese, U., Köster, M., Hassler, U., Martens, U., Trujillo-Barreto, N., Gruber, T., 2013. Successful memory encoding is associated with increased cross-frequency coupling between frontal theta and posterior gamma oscillations in human scalp-recorded EEG. Neuroimage 66, 642–647. https://doi.org/10.1016/j.neuroimage.2012.11.002.

Greenberg, J.A., Burke, J.F., Haque, R., Kahana, M.J., Zaghloul, K.A., 2015. Decreases in theta and increases in high frequency activity underlie associative memory encoding. Neuroimage 114, 257–263. https://doi.org/10.1016/j.neuroimage.2015.03.077.

Griffiths, B., Mazaheri, A., Debener, S., Hanslmayr, S., 2016. Brain oscillations track the formation of episodic memories in the real world. Neuroimage 143, 256–266. https://doi.org/10.1016/J.NEUROIMAGE.2016.09.021.

Hanslmayr, S., Spitzer, B., Bäuml, K.H., 2009. Brain oscillations dissociate between semantic and nonsemantic encoding of episodic memories. Cerebr. Cortex 19, 1631–1640. https://doi.org/10.1093/cercor/bhn197.

Hassler, U., Barreto, N., Gruber, T., 2011. Induced gamma band responses in human EEG after the control of miniature saccadic artifacts. Neuroimage 57.

Helfrich, R.F., Fiebelkorn, I.C., Szczepanski, S.M., Lin, J.J., Parvizi, J., Knight, R.T., Kastner, S., 2018. Neural mechanisms of sustained attention are rhythmic. Neuron 99 (4), 854–865.

Heusser, A.C., Poeppel, D., Ezzyat, Y., Davachi, L., 2016. Episodic sequence memory is supported by a theta–gamma phase code. Nat. Neurosci. 19, 1374–1380. https://doi.org/10.1038/nn.4374.

Jensen, O., Mazaheri, A., 2010. Shaping Functional Architecture by Oscillatory Alpha Activity: Gating by Inhibition. Front. Hum. Neurosci. 4, 1–8. https://doi.org/10.3389/fnhum.2010.00186.

Kaspar, K., Hassler, U., Martens, U., Trujillo-Barreto, N., Gruber, T., 2010. Steady-state visually evoked potential correlates of object recognition. Brain Res. 1343, 112–121. https://doi.org/10.1016/j.brainres.2010.04.072.

Klimesch, W., 2012. Alpha-band oscillations, attention, and controlled access to stored information. Trends Cognit. Sci. 16, 606–617. https://doi.org/10.1016/j.tics.2012.10.007.

Klimesch, W., 1999. EEG alpha and theta oscillations reflect cognitive and memory performance: A review and analysis. Brain Res. Rev. 29, 169–195. https://doi.org/10.1016/S0165-0173(98)00056-3.

Köster, M., Finger, H., Graetz, S., Kater, M., Gruber, T., 2018. Theta-gamma coupling binds visual perceptual features in an associative memory task.

Köster, M., Finger, H., Kater, M.-J., Schenk, C., Gruber, T., 2017a. Neuronal Oscillations Indicate Sleep-dependent Changes in the Cortical Memory Trace. J. Cognit. Neurosci. 29, 698–707. https://doi.org/10.1162/jocn_a_01071.

Köster, M., Friese, U., Schöne, B., Trujillo-Barreto, N., Gruber, T., 2014. Theta-gamma coupling during episodic retrieval in the human EEG. Brain Res. 1577, 57–68. https://doi.org/10.1016/j.brainres.2014.06.028.

Köster, M., Haese, A., Czernochowski, D., 2017b. Neuronal oscillations reveal the processes underlying intentional compared to incidental learning in children and young adults. PLoS One 12. https://doi.org/10.1371/journal.pone.0182540.

Landau, A.N., Schreyer, H.M., Van Pelt, S., Fries, P., 2015. Distributed Attention Is Implemented through Theta-Rhythmic Gamma Modulation. Curr. Biol. 25, 2332–2337. https://doi.org/10.1016/j.cub.2015.07.048.

Lisman, J.E., Jensen, O., 2013. The Theta-Gamma Neural Code. Neuron 77, 1002–1016. https://doi.org/10.1016/j.neuron.2013.03.007.

Lowet, E., Roberts, M.J., Bosman, C.A., Fries, P., de Weerd, P., 2016. Areas V1 and V2 show microsaccade-related 3-4-Hz covariation in gamma power and frequency. Eur. J. Neurosci. 43, 1286–1296. https://doi.org/10.1111/ejn.13126.

Marshall, L., Helgadóttir, H., Mölle, M., Born, J., 2006. Boosting slow oscillations during sleep potentiates memory. Nature 444, 610–613. https://doi.org/10.1038/nature05278.

Müller, M., Malinowski, P., Gruber, T., Hillyard, S., 2003. Sustained division of the attentional spotlight. Nature 424.

Ngo, H.V.V., Martinetz, T., Born, J., Mölle, M., 2013. Auditory closed-loop stimulation of the sleep slow oscillation enhances memory. Neuron 78, 545–553. https://doi.org/10.1016/j.neuron.2013.03.006.

Osipova, D., Takashima, A., Oostenveld, R., Fernandez, G., Maris, E., Jensen, O., 2006. Theta and Gamma Oscillations Predict Encoding and Retrieval of Declarative Memory. J. Neurosci. 26, 7523–7531. https://doi.org/10.1523/JNEUROSCI.1948-06.2006.

Pavlides, C., Greenstein, Y.J., Grudman, M., Winson, J., 1988. Long-term potentiation in the dentate gyrus is induced preferentially on the positive phase of θ-rhythm. Brain Res. 439, 383–387. https://doi.org/10.1016/0006-8993(88)91499-0.

Sederberg, P.B., Kahana, M.J., Howard, M.W., Donner, E.J., Madsen, J.R., 2003. Theta and gamma oscillations during encoding predict subsequent recall. J. Neurosci. 23, 10809–10814. https://doi.org/23/34/10809 [pii].

Squire, L.R., Zola-morgan, S., 1991. The Medial Temporal Lobe Memory System. Science (80-) 253, 1380–1386. https://doi.org/10.1126/science.1896849.

Staudigl, T., Hanslmayr, S., 2013. Theta oscillations at encoding mediate the context-dependent nature of human episodic memory. Curr. Biol. 23, 1101–1106. https://doi.org/10.1016/j.cub.2013.04.074.

Spyropoulos, G., Bosman, C.A., Fries, P., 2018. A theta rhythm in macaque visual cortex and its attentional modulation. Proc. Natl. Acad. Sci. Unit. States Am. https://doi.org/10.1073/pnas.1719433115, 201719433.

Tort, A.B.L., Komorowski, R., Eichenbaum, H., Kopell, N., 2010. Measuring phase-amplitude coupling between neuronal oscillations of different frequencies. J. Neurophysiol. 104, 1195–1210. https://doi.org/10.1152/jn.00106.2010.

Tulving, E., 1995. Organization of Memory: Quo Vadis? Cognit. Neurosci., 839847. https://doi.org/10.1017/S0140525X00047257.

VanRullen, R., 2016. Perceptual Cycles. Trends Cognit. Sci. 20. https://doi.org/10.1016/j.tics.2016.07.006.

Vosskuhl, J., Huster, R.J., Herrmann, C.S., 2015. Increase in short-term memory capacity induced by down-regulating individual theta frequency via transcranial alternating current stimulation. Front. Hum. Neurosci. 9. https://doi.org/10.3389/fnhum.2015.00257.

Yuval-Greenberg, S., Tomer, O., Keren, A.S., Nelken, I., Deouell, L.Y., 2008. Transient Induced Gamma-Band Response in EEG as a Manifestation of Miniature Saccades. Neuron 58, 429–441. https://doi.org/10.1016/j.neuron.2008.03.027.